One-Pot Synthesis of PEGylated Ultrasmall Iron-Oxide Nanoparticles and Their in Vivo Evaluation as Magnetic Resonance Imaging Contrast Agents

Jean-François Lutz,*,† Sabrina Stiller,† Ann Hoth,† Lutz Kaufner,‡ Ulrich Pison,‡ and Régis Cartier*,‡

Research Group Nanotechnology for Life Science, Fraunhofer Institute for Applied Polymer Research, Geiselbergstrasse 69, Potsdam 14476, Germany, and Charité, Universitätsmedizin Berlin, Spandauer Damm 130, 14050 Berlin, Germany

Received August 2, 2006; Revised Manuscript Received September 7, 2006

A well-defined copolymer poly(oligo(ethylene glycol) methacrylate-*co*-methacrylic acid) P(OEGMA-*co*-MAA) was studied as a novel water-soluble biocompatible coating for superparamagnetic iron oxide nanoparticles. This copolymer was prepared via a two-step procedure: a well-defined precursor poly(oligo(ethylene glycol) methacrylate-*co*-*tert*-butyl methacrylate), P(OEGMA-*co*-*t*BMA) ($M_n = 17300$ g mol^{-1}; $M_w/M_n = 1.22$), was first synthesized by atom-transfer radical polymerization in the presence of the catalyst system copper(I) chloride/2,2′-bipyridyl and subsequently selectively hydrolyzed in acidic conditions. The resulting P(OEGMA-*co*-MAA) was directly utilized as a polymeric stabilizer in the nanoparticle synthesis. Four batches of ultrasmall PEGylated magnetite nanoparticles (i.e., with an average diameter below 30 nm) were prepared via aqueous coprecipitation of iron salts in the presence of variable amounts of P(OEGMA-*co*-MAA). The diameter of the nanoparticles could be easily tuned in the range 10−25 nm by varying the initial copolymer concentration. Moreover, the formed PEGylated ferrofluids exhibited a long-term colloidal stability in physiological buffer and could therefore be studied in vivo by magnetic resonance (MR) imaging. Intravenous injection into rats showed no detectable signal in the liver within the first 2 h. Maximum liver accumulation was found after 6 h, suggesting a prolongated circulation of the nanoparticles in the bloodstream as compared to conventional MR imaging contrast agents.

Introduction

Magnetic nanoparticles have been recently extensively studied and applied in the biomedical field.[1,2] For instance, iron oxide nanoparticles made of either magnetite (Fe_3O_4) or maghemite (γ-Fe_2O_3) have been widely investigated as contrast agents for magnetic resonance (MR) imaging.[3] As a result, several commercial products based on superparamagnetic iron oxide particles are currently available for human diagnostics. Such commercial nanoparticles are typically coated by a biocompatible polymer (e.g., poly(vinyl alcohol) or dextran), which improves their colloidal stability in physiological media and significantly reduces their toxicity. However, the in vivo half-life time of these polymer-modified nanoparticles is usually rather short. A few minutes after intravenous delivery, the particles are selectively captured by the reticuloendothelial system and efficiently cleared out of the bloodstream. Hence, the range of application of superparamagnetic iron oxide particles remains so far mostly limited to spleen and liver diagnostics.[4,5]

In this context, broadening the in vivo capabilities of iron oxide nanoparticles is a stimulating scientific challenge. For example, it would be interesting to develop magnetic nanoparticles able to combine both drug delivery and diagnostics potentials.[6] However, for reaching such a goal, the circulation time of iron oxide particles should be indeed prolonged if a systemic application is desired. Several works already illustrated that the behavior of magnetic nanoparticles in the bloodstream depends closely on their nanoscale morphology (e.g., overall diameter, size distribution, or nature of the surface).[7,8] For instance, ultrasmall superparamagnetic nanoparticles (i.e., particles with an average diameter below 30 nm) exhibit typically a longer half-life time in blood than larger nanoparticles.[6,7,9] In addition, the surface modification of iron oxide nanoparticles was evidenced to be a versatile strategy for controlling their biological performances (e.g., for reducing their immunogenicity or for promoting targeted delivery to specific tissues).[6,8,10−18] However, the overall correlation between nanoparticles morphology and in vivo behavior remains so far rather obscure.

Various types of organic or inorganic materials can be utilized for modifying the surfaces of iron oxide nanoparticles.[13] In particular, as mentioned above, special attention has been paid to water-soluble polymers, which generally lead to robust biocompatible surface coatings.[19−24] However, rather simple surface modifications have been described so far in the literature (i.e., in most of the reported works, ill-defined commercial homopolymers have been used for modifying the particles). A more advanced surface engineering is undoubtedly necessary for controlling the in vivo fate of magnetic nanoparticles. Such goal seems attainable given the recent progress in macromolecular chemistry. In particular, the recent development of control radical polymerization (CRP) methods such as atom-transfer radical polymerization (ATRP), nitroxide-mediated polymerization (NMP), or reversible addition-fragmentation transfer polymerization (RAFT) considerably broadened the field of macromolecular engineering.[25−28] Indeed, CRP techniques

* To whom correspondence should be addressed. E-mail: lutz@iap.fhg.de; rcartier@gmx.de.

† Fraunhofer Institute for Applied Polymer Research.

‡ Universitätsmedizin Berlin.

10.1021/bm0607527 CCC: $33.50 © 2006 American Chemical Society
Published on Web 10/25/2006

Scheme 1. Experimental Pathways Studied for the Preparation of Well-Defined Copolymers (Top) and Iron Oxide Nanoparticles (Bottom)

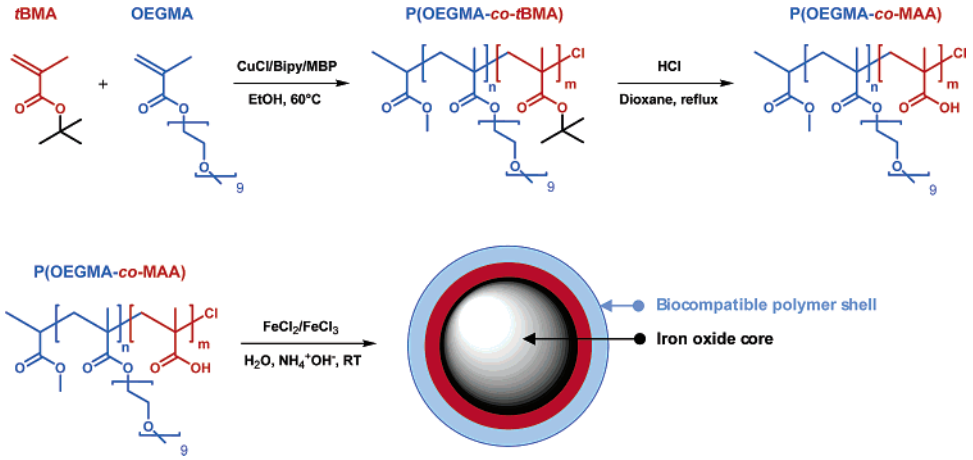

allow preparation of a wide variety of novel tailor-made macromolecules with controlled chain length, composition, functionality, and architecture.[29−34] Moreover, these techniques have been evidenced to be straightforward tools for modifying inorganic surfaces.[35−38] For instance, surface-initiated NMP or ATRP have already been explored for growing polymer brushes on iron oxide nanoparticles.[15,39−45] Alternatively, biocompatible polymer coatings were also obtained by surface adsorption of well-defined copolymers prepared by ATRP (self-assembly approach).[17,46]

In the present work, we investigated a simple one-pot process for constructing ultrasmall biocompatible iron oxide particles (Scheme 1). In this approach, well-defined copolymers poly(oligo(ethylene glycol) methacrylate-*co*-methacrylic acid) prepared by CRP were utilized for functionalizing magnetic nanoparticles. The role of the methacrylic acid units in the copolymer was to interact with the surfaces of the iron oxide particles, whereas the oligo(ethylene glycol) segments were selected for enhancing the water solubility and the biocompatibility of the colloids.[47,48] Moreover, to prepare particles with an overall diameter smaller than 30 nm, the copolymer was used as a stabilizer during the synthesis of the particles. This strategy was recently evidenced to be a straightforward pathway for controlling the size of nanoparticles prepared via conventional precipitation techniques.[46,49] The colloidal properties of the particles in both pure water and physiological medium (i.e., physiological pH and salt concentration) were investigated by dynamic light scattering, zeta potential measurements, and transmission electron microscopy. Additionally, the overall biocompatibility and the blood clearance activity of these ultrasmall particles were investigated by MR imaging on live rat models.

Experimental Section

Materials for Polymer and Particle Synthesis. *tert*-Butyl methacrylate (Aldrich, 98%), oligo(ethylene glycol) methyl ether methacrylate (Aldrich, M_n = 475 g·mol^{-1}), methyl 2-bromopropionate (MBP) (Aldrich, 98%), 2,2′-bipyridyl (Bipy) (Fluka, 98%), ferric chloride hexahydrate ($FeCl_3$·$6H_2O$, Fluka), ferrous chloride tetrahydrate ($FeCl_2$·$4H_2O$, Fluka), ammonium hydroxide solution (Fluka), and fuming hydrochloric acid (Merck) were used as received. Copper(I) chloride (Acros, 95%) was washed with glacial acetic acid to remove any soluble oxidized species, filtered, washed with ethanol, and dried.

Synthesis of Well-Defined Poly(OEGMA-*co*-*t*BMA) via Atom-Transfer Radical Copolymerization. Copper chloride (70 mg, 0.70 mmol) and 2,2′-bipyridyl (218 mg, 1.40 mmol) were added to a Schlenk tube sealed with a septum. The tube was purged with dry argon for a few minutes. Then a degassed mixture of *tert*-butyl methacrylate (3.96 g, 28 mmol), oligo(ethylene glycol) methyl ether methacrylate (20 g, 42 mmol), and 2.4 mL of ethanol was added through the septum with a degassed syringe. Last, methyl 2-bromopropionate (117.5 mg, 0.70 mmol) was added with a microliter syringe. The mixture was heated at 60 °C in an oil bath for 3 h. After several hours, the experiment was stopped by opening the flask and exposing the catalyst to air. The final mixture was diluted in ethanol and passed through a short silica column (60−200 mesh) to remove copper catalyst. Then the filtered solution was diluted with deionized water and subsequently purified by dialysis in water (Roth, ZelluTrans membrane, molecular weight cutoff: 4000−6000). Last, water was removed by azeotropic distillation with ethanol. The purified polymer appeared as a yellowish rubbery material.

Selective Hydrolysis of Poly(OEGMA-*co*-*t*BMA) into Poly(OEGMA-*co*-MAA).[50] Twenty grams of poly(OEGMA-*co*-*t*BMA) and 180 mL of dioxane were added in a round-bottom flask. The mixture was stirred for 10 min to dissolve the polymer. Then 10 mL of concentrated HCl (37%) was added and the flask was capped with a condenser. The mixture was refluxed for approximately 6 h and subsequently cooled to room temperature. Then the filtered solution was diluted with deionized water and subsequently purified by dialysis in water (Roth, ZelluTrans membrane, molecular weight cutoff: 4000−6000). Last, water was removed by rotary evaporation. The purified polymer appeared as a brownish rubbery material.

General Procedure for the One-Step Preparation of PEGylated Fe_3O_4 Nanoparticles. The magnetic nanoparticles were synthesized via a conventional precipitation method in the presence of the copolymer poly(OEGMA-*co*-MAA), used as a particle stabilizer. Iron(II) chloride and iron(III) chloride ($[FeCl_3]_0/[FeCl_2]_0$ = 2) were added in a round-bottom flask under an argon atmosphere and were subsequently diluted in deionized water (overall iron concentration in water was approximately 6 g L^{-1}). Then poly(OEGMA-*co*-MAA) was dissolved in the reaction mixture (this step was made under argon flow). The clear orange solution was stirred for several minutes for dissolving the polymer. Last, the ammonium hydroxide solution (25% in H_2O) was slowly added (one drop every 5 s) under strong stirring conditions, resulting in the formation of a dark precipitate. The obtained ferrofluid was subsequently purified by dialysis in deionized water (Roth, ZelluTrans membrane, molecular weight cutoff: 50000). After dialysis, the concentration of the iron particle in water was characterized by gravimetric analysis and adjusted to 2 g L^{-1} by rotary evaporation.

Polymer Characterization. *Size Exclusion Chromatography, SEC.* Molecular weights and molecular weight distributions were determined by SEC performed at 25 °C in tetrahydrofuran (THF) as eluent, using three 5 μ-MZ-SDV columns with pore sizes of 10^3, 10^5, and 10^6 Å (flow rate 1 mL min^{-1}). The detection was performed with a RI-(Shodex RI-71) and a UV-Detector (TSP UV 1000, 260 nm). For calibration, linear polystyrene standards (PSS, Germany) were used.

Table 1. Properties of the Copolymer Poly(OEGMA-*co*-*t*BMA) Prepared by ATRP[a]

$[OEGMA]_0$	$[tBMA]_0$	$[MBP]_0$	*t* (h)	conv. OEGMA[b]	conv. *t*BMA[b]	M_n[c]	M_{nth}[d]	M_w/M_n[c]
60 equiv	40 equiv	1 equiv	17	0.74	0.83	17300	25800	1.22

[a] Experimental conditions: 60 °C; in ethanol solution (monomer/ethanol ~ 1:1 (v/v)); $[MBP]_0/[CuCl]_0/[Bipy]_0 = 1/1/2$. [b] Monomer conversions measured by ^{1}H NMR. [c] Measured by SEC in THF. [d] $M_{nth} = 475$ conv.$_{OEGMA}$ $[OEGMA]_0/[MBP]_0 + 142$ conv.$_{tBMA}$ $[tBMA]_0/[MBP]_0$.

^{1}H NMR. ^{1}H NMR spectra were recorded in either $CDCl_3$ or D_2O on a Bruker DPX-400 operating at 400.1 MHz. Monomer conversions were calculated from ^{1}H NMR spectra in $CDCl_3$ by comparing the integrations of the vinyl protons of the remaining monomers to the integration of specific regions of the formed polymers.

Cloud Point Measurements. The cloud point of the copolymer in water was measured on a Tepper TP1 photometer (Mainz, Germany). Transmittance of polymer solutions in deionized water at 670 nm was monitored as a function of temperature (cell path length: 12 mm; one heating/cooling cycle at rate of 1 °C min^{-1}).

Nanoparticle Characterization. *Dynamic Light Scattering (DLS).* Dynamic light scattering measurements were performed with a Malvern Instruments particle sizer (HPPS-ET 5002) (Malvern Instruments, UK) equipped with a He−Ne laser ($\lambda = 632.8$ nm). The scattering data were recorded at (25 ± 0.1 °C) in backscattering mode at a scattering angle of 173°. Forty microliters of the samples was diluted with 1000 μL of filtrated water (the cutoff of the filter was 0.45 μm) and placed in a 10 × 10 mm quartz cuvette.

Zeta Potential Measurements. The zeta potential of the nanoparticles was determined with a Zetamaster (Malvern Instruments) from an average of five measurements. (For those measurements, 400 μL of a sample was diluted with 4.6 mL of a millimolar sodium chloride solution of pH 7.4.)

Transmission Electron Microscopy. TEM images were obtained using a Zeiss EM 912 Omega microscope at an acceleration voltage of 120 kV.

In Vivo Magnetic Resonance Imaging. Animal studies were performed using adult male Wistar rats (220−250 g, Harlan Winkelmann, Borchen, Germany) following the general guidelines of the German National Institute of Health Care (LAGetSi). Animals were anaesthetized by Sevoflurane (Baxter, Deerfield, IL) inhalation followed by intraperitoneal injection of 90 mg/kg of body weight of ketamine hydrochloride (Serumwerk, Bernburg, Germany) and 10 mg/kg of body weight of xylazine hydrochloride 2% (Bayer, Brunsbüttel, Germany). For repetitive narcosis animals were given 30 and 3 mg/kg of body weight of ketamine and xylazine hydrochloride, respectively. Nanoparticles were applied in a concentration of 0.6 mg of Fe/kg of body weight in 500 μL of 0.9% NaCl solution through intravenous injection into a tail vein and animals were scanned at the indicated time points. MR Imaging was realized using a 3 T-MR scanner (Signa Excite 3.0T, General Electric Healthcare, Milwaukee, WI) equipped with a quadrature extremity coil (diameter of 10 cm, Rapid Biomedical, Würzburg, Germany). The scanning protocol included a fat-suppressed T2-weighted fast spin−echo (FSE) sequence with a repetition time (TR) of 3500 ms, an echo time (TE) of 30 ms, and an echo train length (ETL) of 12. With use of a field-of-view (FOV) of 10 cm × 5 cm and a matrix of 384 × 384, an in-plane resolution of 0.26 × 0.13 mm and a slice thickness of 2 mm were chosen for the 10-cm coil and 3 cm for the 18-cm coil (receiver bandwidth 31.2 kHz). Following this protocol, 9 axial liver slices were taken with four acquisitions within a scan time of 3:51 min.

Results and Discussion

The water-soluble copolymer poly(oligo(ethylene glycol) methacrylate-*co*-methacrylic acid), P(OEGMA-*co*-MAA), was studied as a surfactant for controlling the overall morphology (i.e., both surface and size) of iron oxide nanoparticles prepared by coprecipitation techniques. Such copolymer can be simply prepared by direct radical copolymerization of OEGMA and MAA in either THF, pure water, or water/ethanol mixtures.[51,52] However, such conventional polymerization methods typically lead to ill-defined polymer samples with a broad molecular weight distribution and a heterogeneous chain-to-chain composition. The latter should be preferentially avoided if one wants to prepare monodisperse nanoparticles. Indeed, nanoscale morphologies generally depend on the homogeneity of their molecular building blocks.[53−55] Hence, we investigated herein a two-step synthetic route for preparing well-defined copolymers P(OEGMA-*co*-MAA) with controlled chain length, molecular weight distribution, and composition (Scheme 1).

A well-defined precursor poly(oligo(ethylene glycol) methacrylate-*co*-*tert*-butyl methacrylate), P(OEGMA-*co*-*t*BMA), was first synthesized by ATRP in the presence of the catalyst system CuCl/bipy (methacrylic acid cannot be directly used as a monomer in ATRP since its acid functions interact with the polymerization catalyst).[55] In this experiment, the initial monomer ratio contained 60% OEGMA and 40% *t*BMA. This particular composition was selected for (i) having a fraction of MAA units in the final copolymer sufficient enough for stabilizing the nanoparticles and (ii) having a copolymer principally composed of biocompatible oligo(ethylene glycol) segments (the theoretical weight fraction of OEGMA in the final copolymer is close to 90%). As expected, the formed copolymer P(OEGMA-*co*-*t*BMA) exhibited a narrow molecular weight distribution and a controlled composition (Table 1). However, the experimental number average molecular weight (M_n) measured by SEC was found to be lower than the theoretical value. This behavior is typical of copolymers with a high OEGMA content and is due to the strong differences in hydrodynamic volume between the studied polymer and the linear PS standards used for SEC calibration.[47] Nevertheless, the *t*BMA units in the copolymers were subsequently hydrolyzed under acidic conditions (Scheme 1). ^{1}H NMR measurements of the copolymer before and after HCl treatment confirmed that the hydrolysis is selective for *t*BMA and that the esters of OEGMA are untouched in this deprotection step (Figure 1).[56,57] The resulting well-defined P(OEGMA-*co*-MAA) copolymer possesses a theoretical number average molecular weight of 23000 g mol^{-1} and a MAA content of approximately 35 mol % as measured by ^{1}H NMR. Copolymers P(OEGMA-*co*-MAA) were reported to exhibit in some cases (i.e., depending on the molecular structure) a lower critical solution temperature (LCST) in water.[52] Such behavior is indeed unwanted in the present application since the polymer is expected to be fully water-soluble to temperatures at least as high as 37 °C. Hence, the solution behavior of the P(OEGMA-*co*-MAA) sample in an aqueous medium was studied by turbidimetry (Figure 2). This measurement indicated that the synthesized copolymer exhibited a LCST in pure deionized at 88 °C and therefore confirmed that P(OEGMA-*co*-MAA) can be utilized in vivo. Another important feature of P(OEGMA-*co*-MAA) graft copolymers is indeed their tendency to self-aggregate in aqueous solution.[58,59] This particular behavior is only happening in acidic conditions (i.e., below the pK_a of poly(methacrylic acid)) and was therefore not a drawback in the present study since particle synthesis and in vivo applications are performed in respectively basic and neutral conditions.

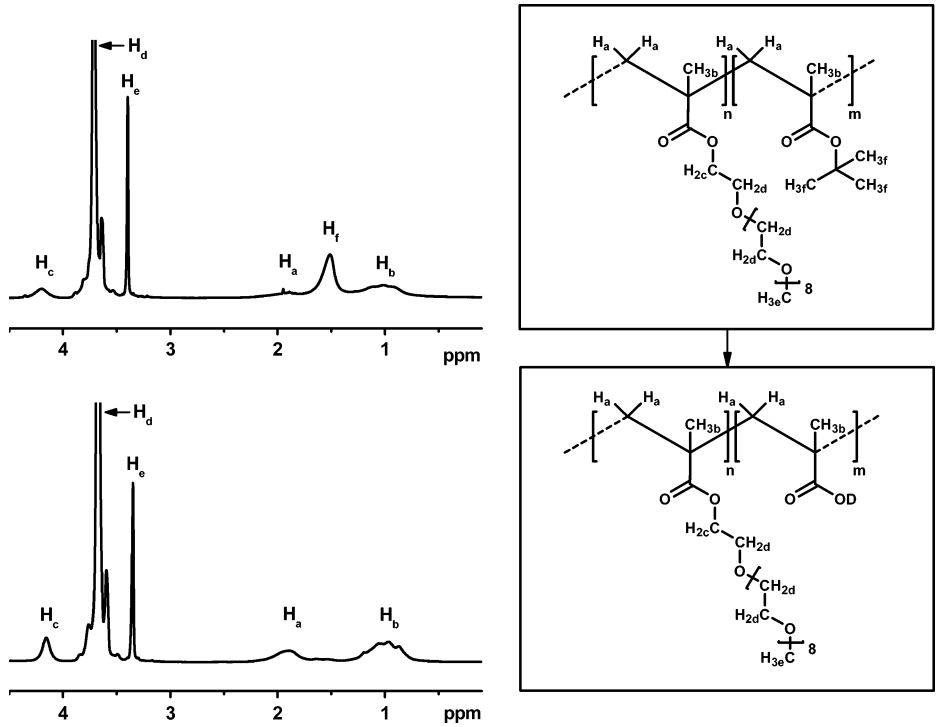

Figure 1. ^{1}H NMR spectra of the well-defined precursor P(OEGMA-*co*-*t*BMA) (top) and its derivative P(OEGMA-*co*-MAA) obtained via selective acid hydrolysis (bottom). Spectra were recorded at room temperature in D_2O.

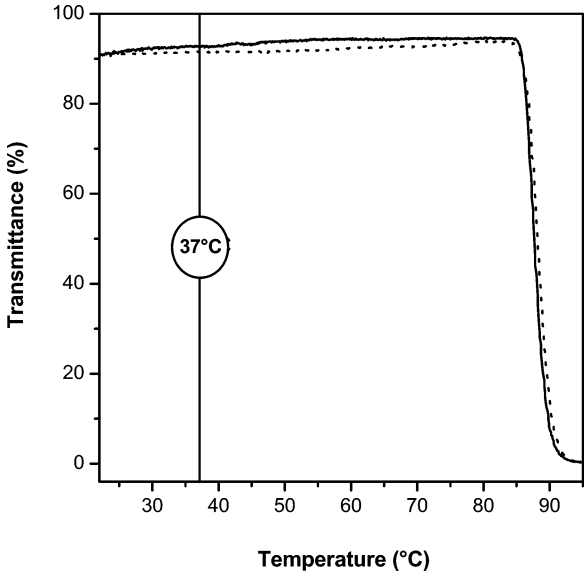

Figure 2. Plots of transmittance as a function of temperature (670 nm, 1 °C min^{-1}) measured for an aqueous solution (3 mg mL^{-1}) of the copolymer P(OEGMA-*co*-MAA) (Table 1). Solid lines: heating cycle; dotted lines: cooling cycle.

Table 2. Properties of the Iron Oxide Nanoparticles Prepared in the Presence of P(OEGMA-*co*-MAA)

	iron salts/ polymer w/w	mean diameter	PDI	ζ
1	1:1	10.1 nm	0.19	−15 mV
2	1:0.85	15.7 nm	0.19	−12 mV
3	1:0.70	18.2 nm	0.37	−7 mV
4	1:0.42	24.3 nm	0.21	−7 mV

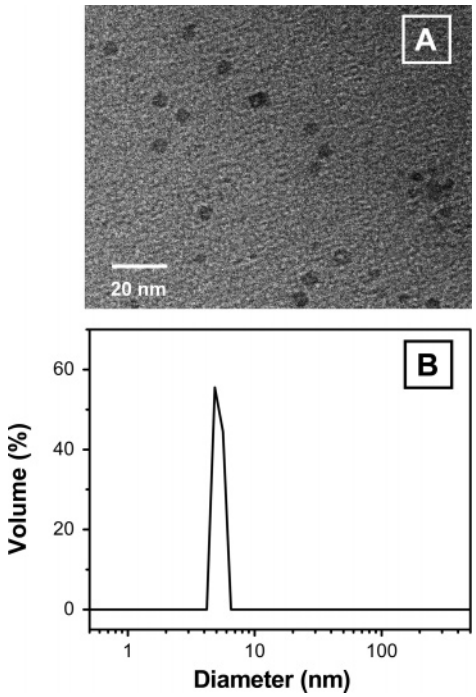

Figure 3. Transmission electron micrograph (A) and size distribution measured by dynamic light scattering (B) for iron oxide nanoparticles prepared in the presence of the copolymer P(OEGMA-*co*-MAA) (Table 2, entry 1).

The iron oxide nanoparticles were synthesized by coprecipitation of ferrous and ferric salts in a basic aqueous solution (a traditional synthetic pathway also sometimes referred to as the method of Massart).[60] This method is experimentally straightforward and has been extensively utilized during the past decades for preparing magnetite ferrofluids. However, the size distribution of the particles prepared is generally rather broad. In comparison, nanoparticles prepared via the thermal decomposition technique recently introduced by Hyeon et al. usually possess a much more defined morphology.[9,61] Nevertheless, a few recent reports indicated that the size and the polydispersity of iron oxide nanoparticles prepared by precipitation methods could be conveniently tuned by adding low molecular weight

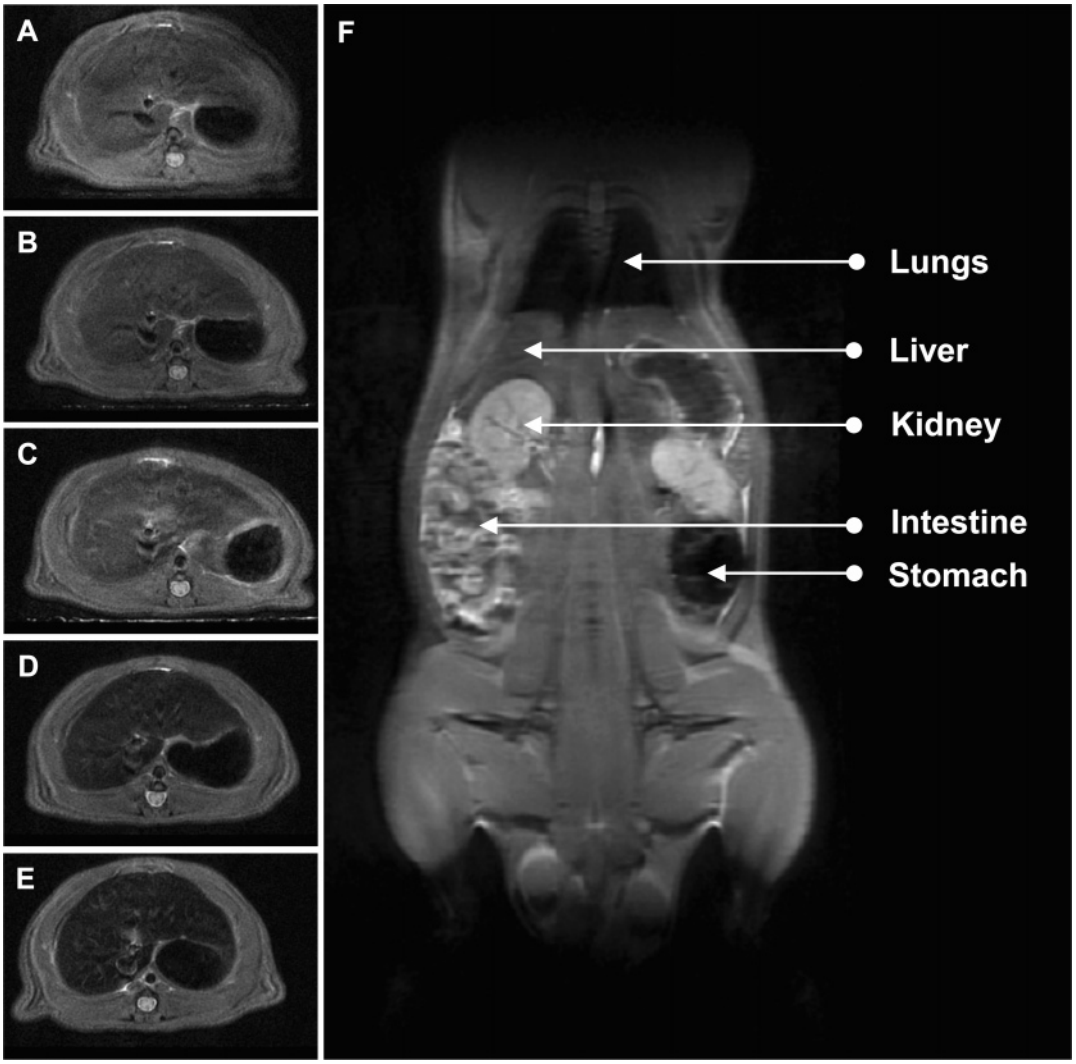

Figure 4. Images of a live rat obtained by magnetic resonance tomography after injection of 500 μL of a solution containing PEGylated iron oxide nanoparticles with an average diameter of 10.1 nm (Table 2, entry 1). Images on the left show liver sections measured at (A) 0 min, (B) 15 min, (C) 1 h, (D) 2 h, and (E) 6 h. Right image shows a coronal section measured after 70 min. Left and right images were measured in two different experiments.

or polymeric cosolutes in the synthetic medium.[23,46,49,62] In particular, Mandal et al. elegantly demonstrated that the diameter of magnetite nanoparticles prepared in the presence of poly(acrylic acid) could be varied in the range 7−14 nm.[49] In this context, it was tempting to use the random copolymer P(OEGMA-*co*-MAA) as a size-control agent in ferrofluid synthesis.

The coprecipitation of iron salts was investigated in the presence of various amounts of P(OEGMA-*co*-MAA) (Table 2). An aqueous mixture of the iron salts and the copolymer was first prepared and ammonium hydroxide was subsequently slowly added to the reaction medium. Shortly after base addition, a dark precipitate, characteristic of iron oxide ferrofluids, was observed in all cases. Due to the presence of P(OEGMA-*co*-MAA) in the synthesis, the formed nanoparticles were found to be indefinitely stable in neutral water. In comparison, nanoparticles prepared in the absence of copolymer (i.e., only stabilized by ammonium hydroxide ion pairs) precipitate immediately when the pH is lowered or when transferred to pure water via dialysis. This behavior confirm the enhanced hydrophilicity of the P(OEGMA-*co*-MAA)-modified nanoparticles. Mandal and co-workers already demonstrated that when used in iron oxide particle synthesis at high pH, the carboxylate anions of polyacids coordinate the iron atoms of magnetite, resulting in the formation of a dense polymer shell on the nanoparticle surfaces.[49] Table 2 describes the four batches of iron oxide nanoparticles prepared in the present work. In all cases, dynamic light scattering evidenced that the diameter of the formed nanoparticles is below 30 nm (i.e., the particles can be ranked as ultrasmall). Moreover, as expected, the overall particle diameter and the size distribution decrease with the initial concentration of P(OEGMA-*co*-MAA) used in the precipitation reaction.[23,49] For the smallest nanoparticles (Table 2, entry 1), the morphology suggested by light scattering measurements was visually confirmed by transmission electron microscopy (Figure 3). The micrograph of Figure 3A shows relatively monodisperse iron oxide nanoparticles possessing a diameter of approximately 7 nm. Zeta potential measurements indicated for all nanoparticles a net negative charge proportional to the amount of polymer utilized during the synthesis, which further confirms the presence of the negatively charged copolymer on the particle surfaces (Table 2).[63] Moreover, the grafting density was estimated for all nanoparticles (assuming a spherical morphology as evidenced by microscopy and a density of 5.05 g cm^{-3} for magnetite) and found to be in the range 0.2−0.3 chains nm^2 in each case. The fact that this number is constant additionally suggests that the experimental diameter of the particles is directly correlated to the amount of polymer involved in the reaction.

All nanoparticle batches were transferred and studied in physiological media (Tris buffered saline solution). In all cases, the iron oxide nanoparticles displayed long-term stability at physiological pH and salt concentration (e.g., no precipitation or coalescence was observed for periods of time as long as 1 month). The overall diameter of all nanoparticle batches was found to be roughly comparable in pure water and physiological medium, whereas the zeta potential decreased by a few mV in physiological conditions.

Overall, the data recorded in the physiological medium suggested that the nanoparticles prepared in the presence of P(OEGMA-*co*-MAA) possess an adequate colloidal stability for being applied in vivo. In previous reports it has been shown that larger iron oxide particles applied through intravenous injection are rapidly recognized by the reticuloendothelial system and, therefore, are displaced from the blood compartment into the liver and spleen.[18] To examine whether the smallest nanoparticles could escape from this clearance process, intravenous injection into the tail vein of living rats was performed and the liver was scanned using MR imaging at different time points after injection. For instance, Figure 4 shows MR imaging liver and coronal sections of an anaesthetized rat recorded after injecting a physiological solution of the smallest iron oxide nanoparticles (Table 2, entry 1). One hour after injection, the liver section of the rat did not show any significant iron accumulation in the liver (the contrast of this organ in Figures 4A and 4C is almost similar). Moreover, the coronal section of the animal (Figure 4F) confirmed that the nanoparticles did not accumulate in other organs (e.g., the kidneys are clear). In comparison, bigger commercial nanoparticles such as Resovist were found to accumulate in the liver approximately 5 min after injection.[18] Such results seem to indicate that the ultrasmall nanoparticles prepared with P(OEGMA-*co*-MAA) have a longer half-life time in the bloodstream than standard commercial contrast agents. These nanoparticles were found to accumulate in the liver after several hours in vivo. After 2 h, the liver was found to be significantly darker (Figure 4D) than the native scan (Figure 4A). After 6 h (Figure 4E), a strong and persistent darkening, corresponding to the maximum contrast signal typically obtained with large particles such as Resovist, could be observed. At this stage, most of the nanoparticles were probably engulfed by the reticuloendothelial system. Nevertheless, it is noteworthy that the in vivo behavior of the PEGylated ultrasmall nanoparticles prepared in the present work is rather different from the one of traditional iron oxide based contrast agents. A complete biological study of the circulation and biodistribution profiles of these promising nanoparticles is currently in progress.

Conclusion

A well-defined biocompatible copolymer composed of methacrylic acid and oligo(ethylene glycol methacrylate) was prepared via a two-step procedure: a copolymer precursor made of *tert*-butyl methacrylate and oligo(ethylene glycol methacrylate) was first synthesized by ATRP in ethanol solution and subsequently selectively hydrolyzed in acidic conditions. The resulting copolymer P(OEGMA-*co*-MAA) exhibited a controlled molecular structure and water solubility up to 88 °C.

This PEGylated polyacid was subsequently studied as a polymeric stabilizer for ferrofluids. Ultrasmall PEGylated magnetite nanoparticles with a tunable diameter (i.e., in the range 10−25 nm) could be prepared via aqueous coprecipitation of iron salts in the presence of different amounts of the copolymer P(OEGMA-*co*-MAA). These nanoparticles exhibited a long-term colloidal stability in either pure deionized water or physiological buffer. The smallest nanoparticles were injected in rats and studied by MR imaging. They did not accumulate in the liver before several hours. Such experimental observation is indirect proof of long circulation in the bloodstream. The biodistribution kinetics of these promising PEGylated ultrasmall nanoparticles is currently under investigation.

Acknowledgment. Fraunhofer society, EU (Project Nano-Carrier No. 2000/2006 2ü/1) and Deutsche Forschungsgemeinschaft (LU 1195/1-1) are greatly acknowledged for financial support. R.C., L.K., and U.P. are grateful to Dr. Harald Bruhn for technical and scientific support in using the MR device at the Radiology Department of the Charité, University Medical School Berlin. Moreover, J.F.L. thanks Professor André Laschewsky (Universität Potsdam) for fruitful discussions.

References and Notes

(1) Rotello, V. M., Ed. *Nanoparticles: Building Blocks for Nanotechnology*; Springer Science: New York, 2004; p 300.
(2) Pankhurst, Q. A.; Connoly, J.; Jones, S. K.; Dobson, J. *J. Phys. D: Appl. Phys.* **2003**, *36*, R167−R181.
(3) Huber, D. L. *Small* **2005**, *1* (5), 482−501.
(4) Stark, D. D.; Weissleder, R.; Elizondo, G.; Hahn, P. F.; Saini, S.; Todd, L. E.; Wittenberg, J.; Ferrucci, J. T. *Radiology (Oak Brook, IL, U.S.)* **1988**, *168*, 297−301.
(5) Hamm, B.; Staks, T.; Taupitz, M.; Maibauer, R.; Speidel, A.; Huppertz, A.; Frenzel, T.; Lawaczeck, R.; Wolf, K. J.; Lange, L. *J. Magn. Reson. Imag.* **1994**, *4*, 659−668.
(6) Neuberger, T.; Schöpf, B.; Hofmann, H.; Hofmann, M.; von Rechenberg, B. *J. Magn. Magn. Mater.* **2005**, *293*, 483−496.
(7) Weissleder, R.; Elidonzo, G.; Wittenberg, J.; Rabito, C. A.; Bengele, H. H.; Josephson, L. *Radiology (Oak Brook, IL, U.S.)* **1990**, *175*, 489−493.
(8) Lewin, M.; Carlesso, N.; Tung, C.-H.; Tang, X.-W.; Cory, D.; Scadden, D. T.; Weissleder, R. *Nat. Biotechnol.* **2000**, *18*, 410−414.
(9) Jun, Y.-W.; Huh, Y.-M.; Choi, J.-s.; Lee, J.-H.; Song, H.-T.; Kim, S.-J.; Yoon, S.; Kim, K.-S.; Shin, J.-S.; Suh, J.-S.; Cheon, J. *J. Am. Chem. Soc.* **2005**, *127* (16), 5732−5733.
(10) Kohler, N.; Fryxell, G. E.; Zhang, M. *J. Am. Chem. Soc.* **2004**, *126* (23), 7206−7211.
(11) Nitin, N.; LaConte, L. E. W.; Zurkiya, O.; Hu, X.; Bao, G. *J. Biol. Inorg. Chem.* **2004**, *9*, 706−712.
(12) Ai, H.; Flask, C.; Weinberg, B.; Shuai, X.-T.; Pagel, M. D.; Farrell, D.; Duerk, J.; Gao, J. *Adv. Mater.* **2005**, *17* (16), 1949−1952.
(13) Gupta, A. K.; Gupta, M. *Biomaterials* **2005**, *26* (18), 3995−4021.
(14) Sonvico, F.; Mornet, S.; Vasseur, S.; Dubernet, C.; Jaillard, D.; Degrouard, J.; Hoebeke, J.; Duguet, E.; Colombo, P.; Couvreur, P. *Bioconjugate Chem.* **2005**, *16* (5).
(15) Hu, F. X.; Neoh, K. G.; Cen, L.; Kang, E.-T. *Biomacromolecules* **2006**, *7* (3), 809−816.
(16) Kohler, K.; Sun, C.; Fichtenholtz, A.; Gunn, J.; Fang, C.; Zhang, M. *Small* **2006**, *2* (6), 785−792.
(17) Lee, H.; Lee, E.; Kim, D. K.; Jang, N. K.; Jeong, Y. Y.; Jon, S. *J. Am. Chem. Soc.* **2006**, *128* (22), 7383−7389.
(18) Thünemann, A. F.; Schutt, D.; Kaufner, L.; Pison, U.; Mohwald, H. *Langmuir* **2006**, *22* (5), 2351−2357.
(19) Lee, J.-H.; Isobe, T.; Senna, M. *J. Colloid Interface Sci.* **1996**, *177*, 490−494.
(20) Mendenhall, G. D.; Geng, Y.; Hwang, J. *J. Colloid Interface Sci.* **1996**, *184*, 519−526.
(21) Butterworth, M. D.; Illum, L.; Davis, S. S. *Colloids Surf., A* **2001**, *79*, 93−102.
(22) Pardoe, H.; Chua-anusorn, W.; St. Pierre, T. G.; Dobson, J. *J. Magn. Magn. Mater.* **2001**, *225*, 41−46.
(23) Wormuth, K. *J. Colloid Interface Sci.* **2001**, *241*, 366−377.
(24) Harris, L. A.; Goff, J. D.; Carmichael, A. Y.; Riffle, J. S.; Harburn, J. J.; St. Pierre, T. G.; Saunders, M. *Chem. Mater.* **2003**, *15* (6), 1367−1377.
(25) Hawker, C. J.; Bosman, A. W.; Harth, E. *Chem. Rev.* **2001**, *101* (12), 3661−3688.
(26) Matyjaszewski, K.; Xia, J. *Chem. Rev.* **2001**, *101* (9), 2921−2990.
(27) Matyjaszewski, K. *Prog. Polym. Sci.* **2005**, *30* (8−9), 858−875.

(28) Perrier, S.; Takolpuckdee, P. *J. Polym. Sci., Part A: Polym. Chem.* **2005**, *43*, 5347−5393.
(29) Coessens, V.; Pintauer, T.; Matyjaszewski, K. *Prog. Polym. Sci.* **2001**, *26* (3), 337−377.
(30) Lacroix-Desmazes, P.; Lutz, J.-F.; Chauvin, F.; Severac, R.; Boutevin, B. *Macromolecules* **2001**, *34* (26), 8866−8871.
(31) Davis, K.; Matyjaszewski, K. *Adv. Polym. Sci.* **2002**, *159*, 1−157.
(32) Lutz, J.-F.; Kirci, B.; Matyjaszewski, K. *Macromolecules* **2003**, *36* (9), 3136−3145.
(33) Lutz, J.-F.; Neugebauer, D.; Matyjaszewski, K. *J. Am. Chem. Soc.* **2003**, *125* (23), 6986−6993.
(34) Lutz, J.-F.; Börner, H. G.; Weichenhan, K. *Macromol. Rapid Commun.* **2005**, *26*, 514−518.
(35) von Werne, T.; Patten, T. E. *J. Am. Chem. Soc.* **1999**, *121* (32), 7409−7410.
(36) Pyun, J.; Matyjaszewski, K. *Chem. Mater.* **2001**, *13* (10), 3436−3448.
(37) Pyun, J.; Kowalewski, T.; Matyjaszewski, K. *Macromol. Rapid Commun.* **2003**, *24*, 1043−1059.
(38) Korth, B. D.; Keng, P.; Shim, I.; Bowles, S. E.; Tang, C.; Kowalewski, T.; Nebesny, K. W.; Pyun, J. *J. Am. Chem. Soc.* **2006**, *128* (20), 6562−6563.
(39) Matsuno, R.; Y., K.; Otsuka, H.; Takahara, A. *Chem. Mater.* **2003**, *15* (1), 3−5.
(40) Wang, Y.; Teng, X.; Wang, J.; Yang, H. *Nano Lett.* **2003**, *3* (6), 789−793.
(41) Marutani, E.; Yamamoto, S.; Ninjbadgar, T.; Tsujii, Y.; Fukuda, T.; Takano, M. *Polymer* **2004**, *45* (7), 2231−2235.
(42) Matsuno, R.; Yamamoto, K.; Otsuka, H.; Takahara, A. *Macromolecules* **2004**, *37* (6), 2203−2209.
(43) Duan, H.; Kuang, M.; Wang, D.; Kurth, D. G.; Möhwald, H. *Angew. Chem., Int. Ed.* **2005**, *44* (11), 1717−1720.
(44) Gravano, S. M.; Dumas, R.; Liu, K.; Patten, T. E. *J. Polym. Sci., Part A: Polym. Chem.* **2005**, *43* (16), 3675−3688.
(45) Gelbrich, T.; Feyen, M.; Schmidt, A. M. *Macromolecules* **2006**, *39* (9), 3469−3472.
(46) Wan, S.; Huang, J.; Yan, H.; Liu, K. *J. Mater. Chem.* **2006**, *16*, 298−303.
(47) Lutz, J.-F.; Hoth, A. *Macromolecules* **2006**, *39* (2), 893−896.
(48) Pasut, G.; Veronese, F. M. *Adv. Polym. Sci.* **2006**, *192*, 95−134.
(49) Si, S.; Kotal, A.; Mandal, T. K.; Giri, S.; Nakamura, H.; Kohara, T. *Chem. Mater.* **2004**, *16* (18), 3489−3496.
(50) Davis, K. A.; Matyjaszewski, K. *Macromolecules* **2000**, *33*, 4039−4047.
(51) Smith, B. L.; Klier, J. *J. Appl. Polym. Sci.* **1998**, *68* (6), 1019−1025.
(52) Jones, J. A.; Novo, N.; Flagler, K.; Pagnucco, C. D.; Carew, S.; Cheong, C.; Kong, X. Z.; Burke, N. A. D.; Stöver, H. D. H. *J. Polym. Sci., Part A: Polym. Chem.* **2005**, *43* (23), 6095−6104.
(53) Förster, S.; Plantenberg, T. *Angew. Chem., Int. Ed.* **2002**, *41* (5), 688−714.
(54) Tu, R. S.; Tirrell, M. *Adv. Drug Del. Rev.* **2004**, *56* (11), 1537−1563.
(55) Lutz, J.-F. *Polym. Int.* **2006**, *55* (9), 979−993.
(56) Jones, M.-C.; Ranger, M.; Leroux, J.-C. *Bioconjugate Chem.* **2003**, *14* (4), 774−781.
(57) Ye, M.; Zhang, D.; Han, L.; Tejada, J.; Ortiz, C. *Soft Matter* **2006**, (3), 243−256.
(58) Mathur, A. M.; Dreschler, B.; Scranton, A. B.; Klier, J. *Nature* **1998**, *392*, 367−370.
(59) Holappa, S.; Kantonen, L.; Winnik, F. M.; Tenhu, H. *Macromolecules* **2004**, *37* (18), 7008−7018.
(60) Massart, R. *IEEE Trans. Magn.* **1981**, *17* (2), 1247−2148.
(61) Hyeon, T.; Lee, S. S.; Park, J.; Chung, Y.; Na, H. B. *J. Am. Chem. Soc.* **2001**, *123* (51), 12798−12801.
(62) Bee, A.; Massart, R.; Neveu, S. *J. Magn. Magn. Mater.* **1995**, *149*, 6−9.
(63) Thünemann, A. F.; Müller, M.; Dautzenberg, H.; Joanny, J.-F.; Löwen, H. *Adv. Polym. Sci.* **2004**, *166*, 113−171.

BM0607527